LIMNOLOGY and OCEANOGRAPHY: METHODS

ASLO

*Limnol. Oceanogr.: Methods* 2024

doi: 10.1002/lom3.10630

# Toward an ecologically realistic experimental system to investigate the multigenerational effects of ocean warming and acidification on benthic invertebrates

**Frédéric Gazeau**,[1]* **Pierre Urrutti**,[1] **Alexandre Dousset**,[2] **Nicolas Brodu**,[3] **Marion Richard**,[4] **Rémi Villeneuve**,[3] **Éric Pruvost**,[1] **Steeve Comeau**,[1] **Hugo Koechlin**,[5] **Fabrice Pernet**[5]

[1]Laboratoire d'Océanographie de Villefranche (LOV), CNRS, Sorbonne Université, Villefranche-sur-Mer, France
[2]Comité Régional de la Conchyliculture de Bretagne Nord (CRCBN), Morlaix, France
[3]Comité Régional de la Conchyliculture de Méditerranée (CRCM), Mèze, France
[4]MARBEC, Univ Montpellier, CNRS, IRD, Ifremer, Sète, France
[5]Laboratoire des Sciences de l'Environnement Marin (LEMAR), Ifremer, Univ Brest, CNRS, IRD, Plouzané, France

## *Abstract*

Human activities over the past 150 yr have led to significant carbon dioxide ($CO_2$) emissions, causing global warming and ocean acidification. Surface ocean temperature has risen by 0.93°C since 1850, with projections of an additional +1.42°C to 3.47°C by 2080–2099. Ocean acidification, driven by $CO_2$ absorption, has already lowered seawater pH by 0.1 units, affecting calcifying organisms, including shelled mollusks. Long-term multigenerational studies on mollusk responses to both ocean acidification and warming, under realistic environmental conditions, are scarce. To address this knowledge gap, two mobile experimental units that can be deployed at the vicinity of shellfish farming areas were developed within the framework of the Cocori$CO_2$ project. The experimental systems were designed to manipulate temperature and pH as offsets from ambient conditions. The experimental units have shown their effectiveness in terms of controlling and maintaining pH and temperature to assess the multigenerational effects of ocean warming and acidification on benthic invertebrates. Finally, the developed experimental systems can be modified easily to provide an educated assessment of the impact of other relevant environmental changes such as deoxygenation and changes in salinity.

Over the past 150 yr, human activities have emitted significant amounts of carbon dioxide ($CO_2$) into the atmosphere through the burning of fossil fuels and land-use changes. This has increased radiative forcing, consequently warming both the atmosphere and the ocean. The surface ocean has warmed by 0.93°C (0.73–1.04°C) from 1850–1900 to 2013 (IPCC 2023). Depending on future emission scenarios, the surface ocean is projected to warm by about 1.42–3.47°C by 2080–2099 relative to 1870–1899 (Kwiatkowski et al. 2020). The ocean not only accumulates a substantial amount of heat, leading to ocean warming, but also absorbs approximately 26% of anthropogenic $CO_2$ emissions (Friedlingstein et al. 2022). This massive input of $CO_2$ significantly impacts seawater carbonate chemistry. Specifically, the increase in $CO_2$ levels lowers the pH of seawater, leading to ocean acidification. The pH of surface ocean waters has already decreased by 0.1 units since the beginning of the industrial era. According to recent projections, a further decrease ranging from 0.16 to 0.44 units is expected by the end of the century, depending on the considered $CO_2$ emission scenario (Kwiatkowski et al. 2020). Ocean acidification also leads to a reduction of the availability of carbonate ions ($CO_3^{2-}$), one of the building blocks of calcium carbonate ($CaCO_3$), and likely alters the ability of calcifying organisms to precipitate $CaCO_3$ (e.g., Gazeau et al. 2013; Albright et al. 2018; Bednaršek et al. 2021). Among calcifiers, shelled marine mollusks appear as one of the most threatened groups (e.g., Kroeker et al. 2013; Gattuso et al. 2015).

The global mollusk industry has experienced rapid growth in recent decades, with aquaculture production representing only 25% of total mollusk consumption in 1950 to almost 90% in 2021. The worldwide mollusk farming industry reached a production of 18.4 million tons in 2021 for a value of ~ 31 billion dollars, representing 15% and 11% of the total

*Correspondence: frederic.gazeau@imev-mer.fr

Additional Supporting Information may be found in the online version of this article.

aquaculture value, respectively (FAO 2022). Mollusk production occurs mostly in marine waters (~ 98.4%) and the Pacific oyster, *Crassostrea gigas*, makes the largest individual contribution (> 30%; FAO 2022).

Being both ecologically and economically important species in the coastal zone, the body of literature on the effects of ocean acidification on shelled mollusks has grown substantially over recent years. While embryos and larvae appear as highly sensitive, evidenced by reductions in growth, survival, and increased developmental time and abnormalities, the response of juveniles and adults to acidification varies both between and within species (Gazeau et al. 2013). This variability impedes the formulation of a comprehensive understanding of the effects of acidification across different life stages.

Direct effects of ocean acidification on the shellfish industry have been observed on the US west coast, more than a decade ago when unprecedented mortality of Pacific oyster larvae occurred. Scientists and shellfish growers jointly found a high correlation between seawater acidity and survival of larvae, clearly linking elevated partial pressure of $CO_2$ ($pCO_2$) or lowered seawater pH to hatchery failures (Barton et al. 2012) which led to the implementation of adaptive strategies (Barton et al. 2015).

Ocean acidification is expected to have clear negative consequences on mollusk farming in terms of net present value, revenue flow or consumer welfare values (Narita et al. 2012; Froehlich et al. 2018; Stewart-Sinclair et al. 2020). However, as for many organisms, our understanding of how mollusk production will evolve in the coming decades is limited by the very small number of long-term (e.g., multigenerational) perturbation experiments. Indeed, most past studies report on experiments where single life history stages of mollusks were exposed to changing conditions for short periods of time (few months at best) and fail to provide clear insights on the future of these species and their exploitation. Only few transgenerational experiments showed that parental effects have been identified as a source of rapid acclimation with the potential to alleviate the impacts of moderately elevated $pCO_2$ (Zhao et al. 2020). However, these studies followed the second generation only for a few weeks under controlled experimental conditions (e.g., Gibbs et al. 2021; Lim et al. 2021). As such, the question whether populations can persist or not in the long term remains fully open. Also, most past perturbation studies exposed coastal organisms to constant conditions based on scenarios modeled for offshore waters. As such, treatments that were aimed at simulating future conditions could have represented present conditions in coastal waters subjected to human pressure and did not reproduce the highly dynamic nature of productive coastal areas (Hofmann et al. 2011; Vargas et al. 2017; Carstensen and Duarte 2019). Finally, ocean acidification and warming are not acting in isolation. It is therefore necessary to consider natural fluctuations in other environmental factors such as oxygen concentration, food level, salinity, turbidity, and living communities in the seawater (plankton, bacteria, viruses).

A better understanding of the effects of ocean acidification and warming on mollusks requires the development of experimental systems allowing the fine control of temperature and pH over long-term experiments supplied with untreated, natural, seawater originating from mollusk farms. Considering this technological gap, we developed ecologically realistic experimental systems to investigate the impacts of ocean acidification and warming over generations of bivalve mollusks. This work is part of an applied, transdisciplinary research project going on with the shellfish industry, funded by the European Maritime and Fisheries Fund (EMFF) between January 2020 and June 2023 (shellfish aquaculture in a high-$CO_2$ world: the Cocori$CO_2$ project). These experimental units consist of two containers deployed on the Atlantic and Mediterranean coasts, two contrasted sites near shellfish farms. Here, we present a technical description and results of preliminary testing of the experimental system deployed in Brittany.

## Materials and methods

### Operational concept of the experimental systems

The experimental units were developed to manipulate and finely control pH and temperature in open-flow tanks containing mollusk species. As there is a strong need to run experiments under realistic (and dynamic) conditions, the tanks and the regulation systems were installed in shipping containers that could be easily deployed on land at the vicinity of shellfish farms. The temperature and pH regulation systems have been designed to offset ambient conditions. With this system, many experimental designs can be considered with relatively few modifications necessary to implement. For the first experiments conducted in the frame of the Cocori$CO_2$ project, it was decided to follow a scenario approach mimicking temperature and pH conditions (both parameters combined) as projected for 2050, 2075, and 2100 according to

**Table 1.** Present (2015–2024) sea surface temperature (SST) and pH on the total scale ($pH_T$) at both study sites as well as offsets projected for the periods 2045–2055, 2070–2080, and 2090–2100 in these regions and for the global surface ocean, according to CMIP6 models following the SSP3-7.0 scenario (Kwiatkowski et al. 2020).

| SSP3-7.0 | | Brittany site | Mediterranean site | Global mean |
|---|---|---|---|---|
| 2015–2024 | SST | 14.42 | 17.79 | – |
| | $pH_T$ | 8.057 | 8.053 | – |
| 2045–2055 | SST | +0.62 | +0.84 | +0.76 |
| | $pH_T$ | −0.11 | −0.10 | −0.10 |
| 2070–2080 | SST | +1.06 | +1.77 | +1.54 |
| | $pH_T$ | −0.21 | −0.19 | −0.19 |
| 2090–2100 | SST | +1.77 | +2.69 | +2.29 |
| | $pH_T$ | −0.29 | −0.26 | −0.26 |

regional outputs from CMIP6 models following the SSP3-7.0 scenario (Kwiatkowski et al. 2020; Table 1). Two containers were developed and deployed in two sites where important shellfish farming activities occur although being very different

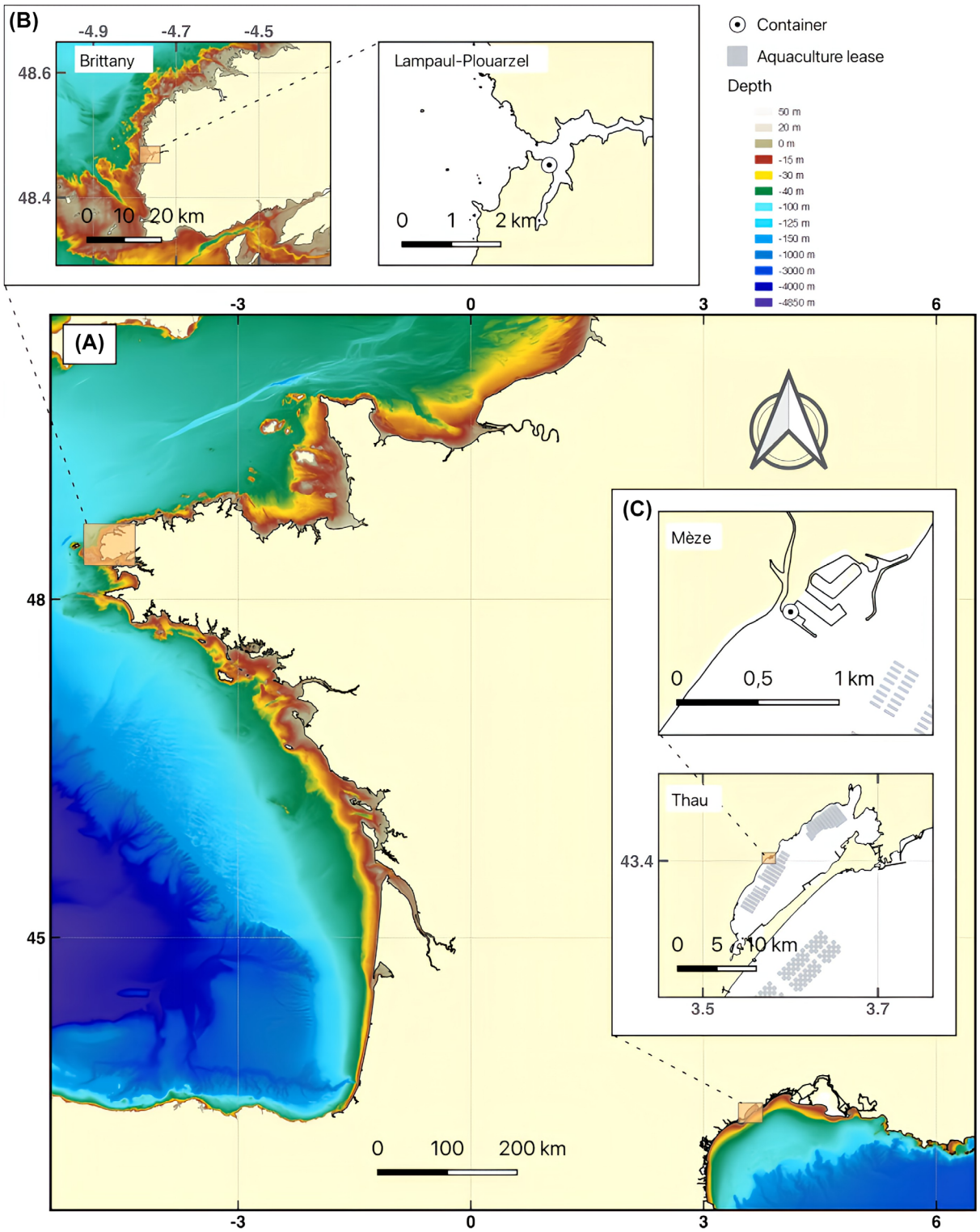


**Fig. 1.** Map of the two deployment areas in France (**A**). The containers were positioned in northern Brittany in Lampaul-Plouarzel (**B**), and in the Mediterranean Thau Lagoon in Mèze (**C**). The precise location of each container is depicted on the high-resolution maps, indicated by the circled dots.

in terms of environmental conditions: on the Atlantic coast in Brittany (annual temperature and salinity ranges: ~ 11–18°C and ~ 31–36, respectively) and in the Mediterranean Sea in the Thau Lagoon (annual temperature and salinity ranges: ~ 7–32°C and ~ 37–42, respectively) where most of the French Mediterranean shellfish production takes place.

The containers were deployed in Brittany within the facilities of the *Centre de Recherche appliquée de Porscave-Comité Régionale de la Conchyliculture de Bretagne Nord* (Lampaul-Plouarzel, France; 48.467°N, 4.7572°W; Fig. 1) and in the Mediterranean area (Thau Lagoon) within the facilities of the *Comité Régionale de la Conchyliculture de Méditerranée* (Mèze, France; 43.4027°N, 3.5760°E; Fig. 1).

In Brittany, tanks were filled with Pacific (cupped; *Crassostrea gigas*) and flat oysters (*Ostrea edulis*) maintained under partially emerged (intertidal) and fully submerged (subtidal) conditions, respectively. In the Mediterranean, Pacific oysters and Mediterranean mussels (*Mytilus galloprovincialis*) were placed in the tanks and reared under fully submerged conditions (no tide).

## Description of the experimental systems

### *General setup*

The two developed experimental units consist of 20-ft air-conditioned shipping containers, equipped with 12 × 250-liter open-flow tanks along with a hydraulic control skid and automation devices to control water temperature and pH. The interior of the containers was insulated and equipped with stainless steel and epoxy painted walls. In each container, four drains were added to the sur-elevated floor to evacuate (sea) water in case of overflows and during cleaning. Three holes were made for hydraulic inlets on the side of the containers for ambient and warmed seawater as well as for freshwater (cleaning). Hydraulic outlets were added on the floor of the containers to allow flow-through seawater to be gravity evacuated through 50-mm diameter pipes. A 3P + N 32A connector was installed above the door, and an electrical cabinet was built with circuit breakers for the power sockets, the air conditioning, the automation cabinet, and the lights. The internal organization of the container was designed using Autodesk Inventor 2022 to fit in all the necessary equipment (Fig. 2). The containers were deployed on the two study sites in September 2021. Supporting Information Table A.1 provides the parts list for the items installed in each container.

### *Hydraulic design*

In Brittany, ambient seawater is provided by two submersible pumps (3153HT, FLYGT©) deployed 1 m below the lowest low tide of the year at a site located 680 m from the container. In the Mediterranean, a submersible pump (Albatros F13T, NPS©) is deployed at a depth of 1 m around 130 m from the container. On both locations, seawater is warmed by heat pumps equipped with a titanium heat exchanger (PAC-2-28T RO 42,3 kW, ETT© and Osmose© in Brittany and in the Mediterranean, respectively) installed outside the containers. In the Mediterranean, the water temperature provided by the heat exchanger is measured and controlled by a motorized analogic three-way valve (R3025-10-S4 + LN24A-SR, Belimo©) to maintain temperature at the desired value. Warmed water temperature is maintained between 20°C and 45°C depending on the site and the period of the year.

At each study site, ambient seawater (a flow rate of maximum 6 $m^3$ $h^{-1}$) and warmed seawater (a flow rate of maximum 3 $m^3$ $h^{-1}$) is delivered to the experimental system with 40-mm diameter PE tubing. Pressure sensors (TP 805-528915-4, Siemens©) for both seawater inlets measure the water pressures and allow motorized analogic two-way valves (R2025-10-S2 + NR24A-SR, Belimo©) to maintain a similar and stable pressure for warmed and ambient seawater (40,000 Pa).

At the entrance of the containers, a non-pressurized 50-liter tank is fed with ambient seawater and holds five sensors to measure key variables: temperature and pH (Polylite Plus PHI ARC 120, Hamilton©), conductivity (PC4EB, Aqualabo©), dissolved oxygen (PODOC, Aqualabo©), fluorescence (Cyclops-7F, Turner Designs©), and turbidity (PNEPB, Aqualabo©).

The three control condition tanks are supplied with ambient seawater. For the three perturbed conditions, the tanks are fed with a mixture of ambient, warmed, and acidified seawater (Fig. 3). The mixture is done in 3 × 50-liter PE pressurized tanks equipped with a pH/temperature sensor (Polylite Plus

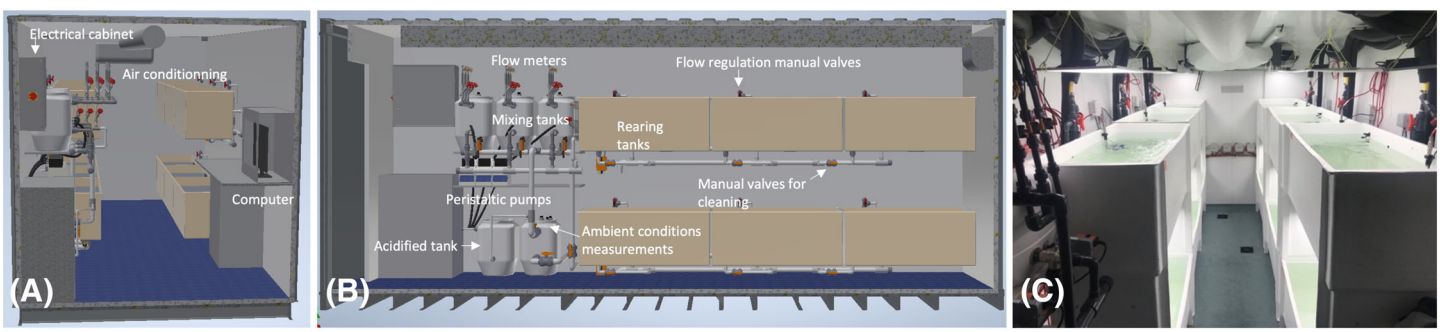


**Fig. 2.** Schematics of a container (**A**: short side view and **B**: long side view) and (**C**) picture of the experimental tanks (without animals).

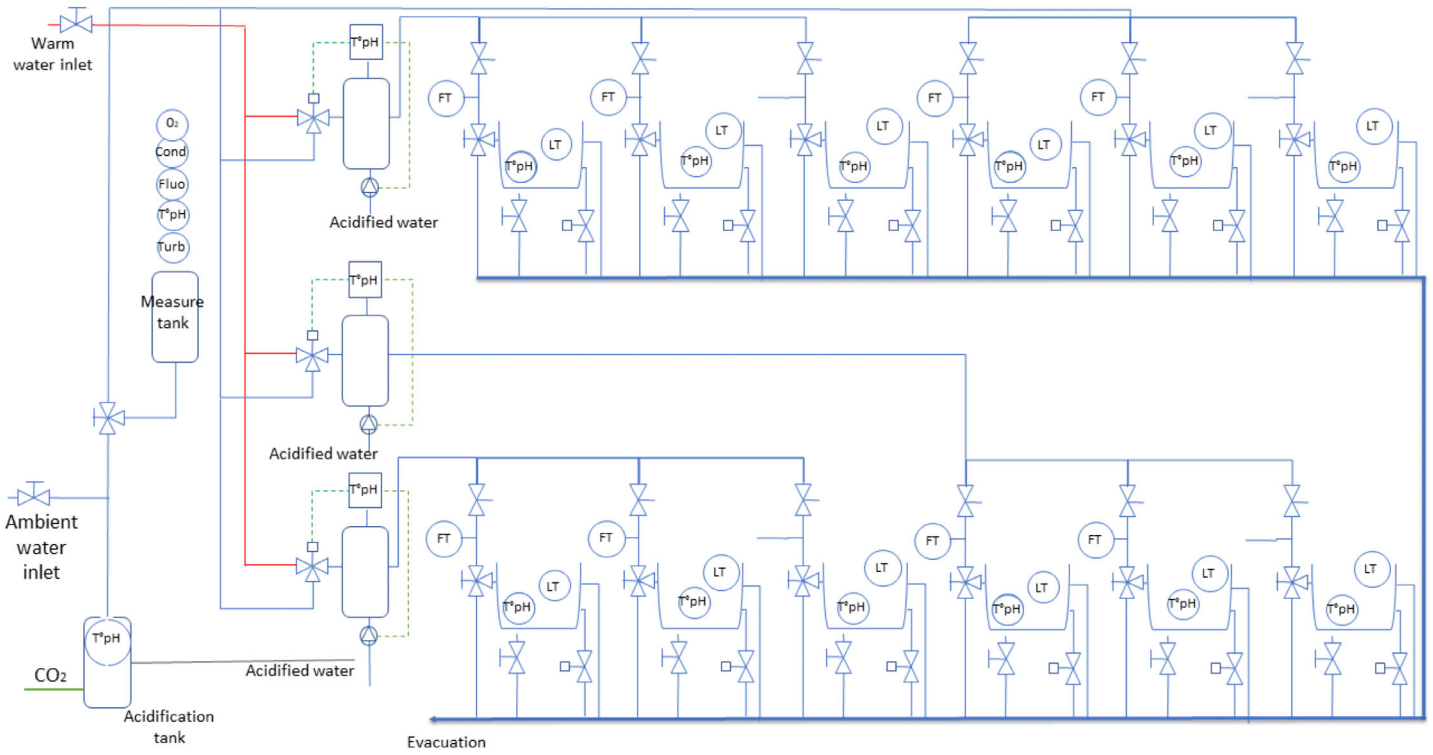


**Fig. 3.** Process and instrumentation diagram (P&ID) of the experimental systems.

PHI ARC 120, Hamilton©). The high flow rate (1.5 $m^3\ h^{-1}$) compared with the small volume of the mixing tanks ensures a homogenous mixing before feeding the rearing tanks. A picture showing the mixing system is provided in Supporting Information Fig. A.1. Directly from the ambient seawater inlet for the control conditions or from these mixing tanks for the warmed/acidified conditions, the 12 rearing tanks receive seawater using insulated flexible hoses at a rate of 0.5 $m^3\ h^{-1}$, corresponding to a complete turnover of seawater in about 30 min. Flow rates are measured using 12 flow meters (SV3150, IFM©) installed on the input pipe of each rearing tank after the mixing tank and are manually set at the appropriate flow rate using manual hand-crank valves positioned at the inlet of each tank. On both sites, after passing through the tanks, seawater evacuated through the hydraulic outlets was flushed at sea with a 50 mm diameter PE tubing.

### *Temperature and pH automatic regulation*

Temperature regulation is achieved using an analogic motorized three-way valve (R3015-4-S1 + LR24A-SR, Belimo©) that adjusts the mixing of warmed and ambient seawater to reach the targeted temperature set point in the corresponding mixing tank based on continuous temperature measurements (PHI ARC 120, Hamilton©). Temperature regulation is performed using a software PID (proportional integral derivative) controller on the corresponding programmable logic controller (PLC), in PoE mode (proportional on error). The PID controller measures the difference between the temperature signal and the set point, and calculates the valve opening by multiplying the error, the integral of the error and the derivative of the error, by previously determined coefficients $K_p$, $K_i$, and $K_d$, respectively. These coefficients were obtained experimentally using the empiric method of (Ziegler and Nichols 1942). They may differ from one condition to another.

The regulation of pH is achieved by bubbling $CO_2$ in a non-pressurized 50-liter PE tank filled with ambient seawater. Seawater addition in this tank is controlled by a two-way valve whose opening is dependent on a float-level switch (Cynergy3, Radiospare©) installed at the top of the tank. The flow of pure $CO_2$ is controlled by an electrovalve (VX210MG, SMC©), and $CO_2$ is bubbled in seawater using a ceramic microbubble diffuser (ECD100, Enviroceramic©). A pH sensor (PHI ARC 120, Hamilton©) continuously measures pH in this tank to maintain pH at a value close to $CO_2$ saturation ($\sim$ 4.9; Supporting Information Fig. A.2). This acidified water is then pumped to the three pressurized mixing tanks using peristaltic pumps (Minipuls3, Gilson©). The rate of the $CO_2$ acidified water delivery to the mixing tanks is adjusted by the PLC to reach the respective pH nominal values based on continuous pH readings in the corresponding pressurized mixing tanks

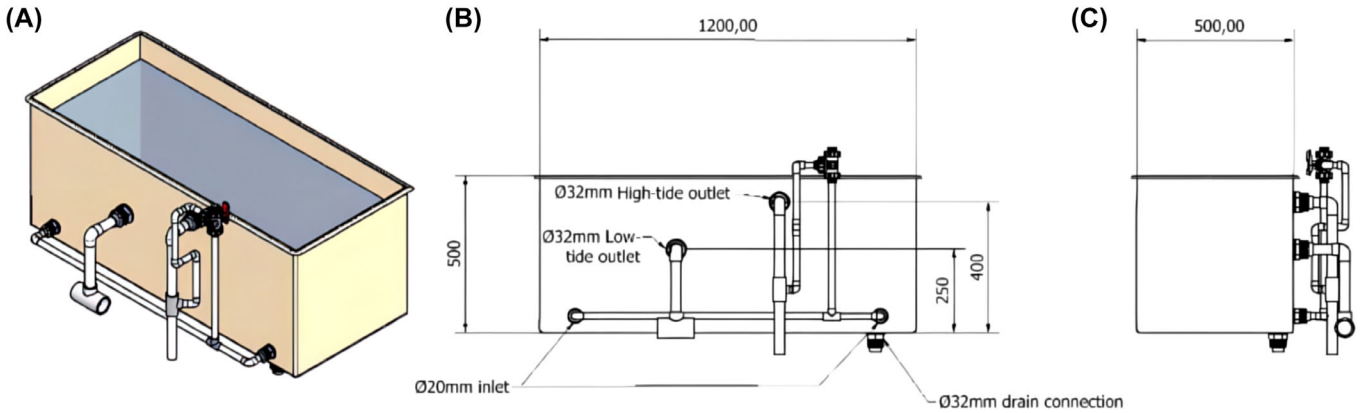


**Fig. 4.** Schematic of a rearing tank (**A**: 3D drawing, **B**: long back side, **C**: short side) showing its dimensions (in mm), as well as the seawater inlets and outlets.

(PHI ARC 120, Hamilton©). As for temperature regulation, a software PID controller ensures the accuracy of the regulation.

***Rearing tanks***

Rearing tanks are parallelepipeds ($L \times l \times H = 120 \times 50 \times 50$ cm, total volume of 300 liters) built in fiberglass and polyester resin (Fig. 4). Longer feet mounted on the top tanks allow stacking them up and access to the lower tanks. Two 20-mm diameter inlets in the bottom back corner of the tanks are used for water inlet. A mid-height 32-mm diameter outlet is used for low-tide water output and a top 32-mm diameter outlet is used for high-tide water output. High and low tide is accomplished by opening or closing an automatic two-way valve (ELV15010, Plombservice©) on the low-tide output pipe. Emersion is made by instantly (2–5 min) emptying half of the water of the tanks. The valve remains open for the whole low- to high-tide time. High-tide and low-tide times are calculated to reproduce the tide period on the actual experiment site. The drainage system is installed in both containers but only active in the Brittany site since there is no significant tide in the Mediterranean.

Three float-level switches (Cynergy3, Radiospare©) allow to monitor critical levels in every tank: (1) high level: float placed 5 cm from the top, to detect an overflow; (2) low level: placed 5 cm above low tide, to make sure the emersion is effective; and (3) very low level: place 15 cm from the bottom, to detect a leak in the tank or a problem with seawater supply.

Each tank is equipped with a temperature and pH sensor (PHI ARC 120, Hamilton©), and with a 12-W wavemaker pump (JVP-132, Sunsun©) to ensure a proper mixing. The sensor is placed below the low-tide level to always keep it immerged. Seawater is evacuated by gravity through the outlet pipes of the container. For maintenance and cleaning purposes, a manual drain valve is installed at the bottom of the tanks to quickly and fully empty them. A manual by-pass valve on the input pipe allows cleaning the whole container piping by flowing freshwater with bleach, without adding bleach to the tanks. Each tank is equipped with a 4200K led ramp (ULED-PANEL 300X1200 BN, Universal LED©) installed 50 cm above the highest surface level and is automatically switched on and off based on the local sunrise and sunset times.

***System cleaning***

Manual valves are disposed under each tank for emptying and cleaning purpose. On the computer, the regulation system can be paused using the "Cleanup" mode. All tanks are cleaned once a week. Mollusks are first removed from the tanks and exposed to air for 1–2 h while an intensive physical brushing in performed with freshwater to remove sediment and biofouling from the sides of the tanks, the mixing pumps, and the pH/temperature electrode.

Once a month, a full cleaning including the mixing tanks and all tubing inside the container is performed with bleach. Outside the container, a 500-liter tank is filled with freshwater and bleach (final concentration of 0.01%). The manual by-pass valve is open and bleached freshwater is sent into the ambient water circuit via a cellar vacuum pump. Around 30 min later, the manual by-pass valve is closed and the system freshwater is flushed from the water circuit by restarting the seawater pump.

***Automation***

All automation equipment is installed in an electrical cabinet (picture provided in Supporting Information Fig. A.3), an IP68 Fibox enclosure with a 400 V (3P + N + E) 32A security switch. All the automation elements use low tension (12 Vdc or 24 Vdc) through circuit breakers and fuses. The 24 VDC power supply is used to power the PLCs, the regulation and drainage valves, the ethernet switch, and the level sensors. The 12 VDC power supply is used to power the fluorescence sensor and the RS485 bus sensors.

The automation of the system is made using four Industrial Arduino-based PLCs (Mduino-21+, Industrial shields©). Each PLC is responsible for the data logging and regulation of a specific treatment (i.e., three tanks each). One PLC Master is also responsible for the communication between PLCs and the

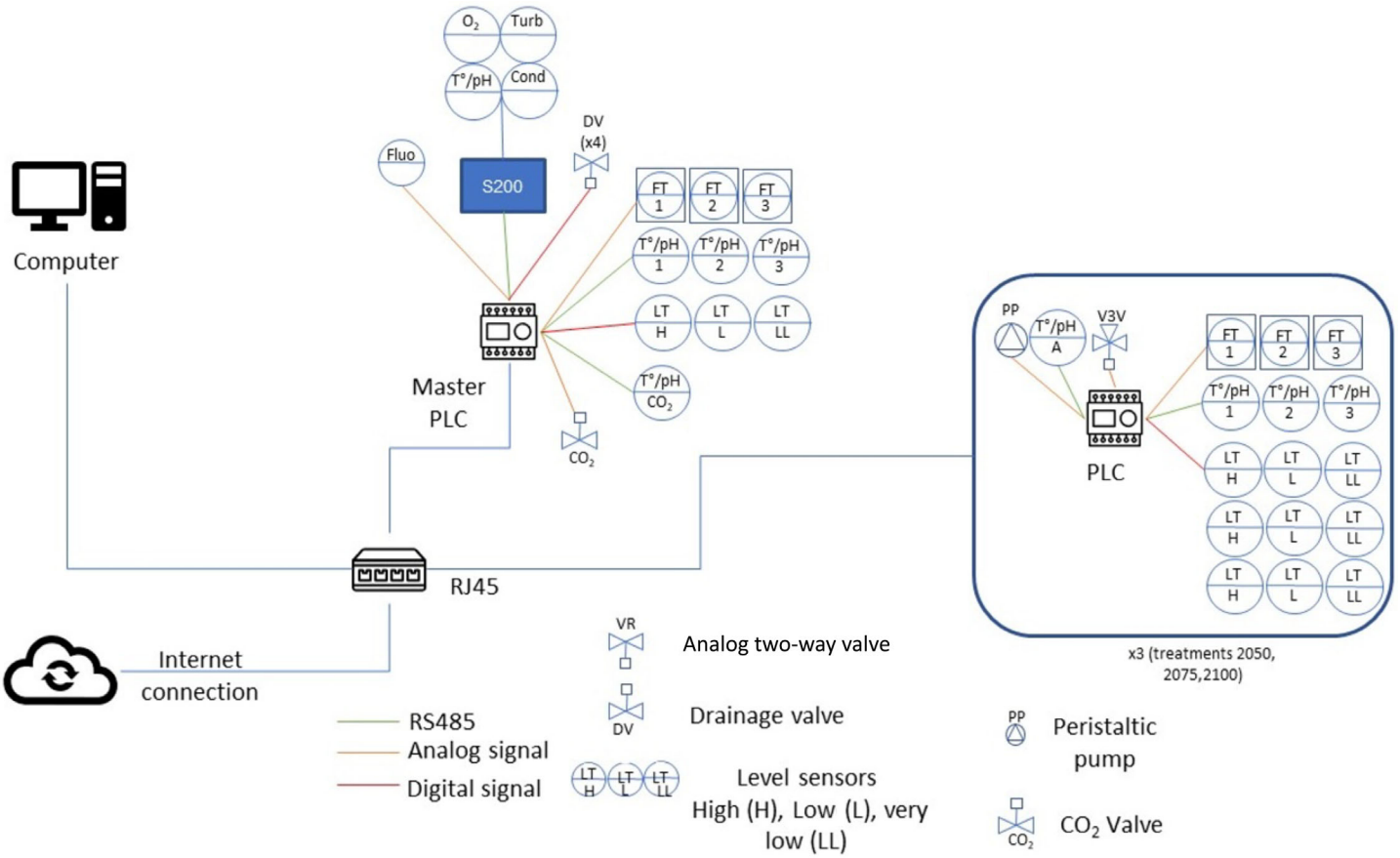


**Fig. 5.** Automation design.

computer. The automation architecture is presented in Fig. 5. The software program of the PLCs is written in C, using Visual Studio 2019, Arduino 1.8.13, and the vMicro plugin to allow Arduino code compilation and upload.

The monitoring computer runs a Windows application developed in C#, responsible for reading data received from the PLCs, sending settings and commands to the PLCs, displaying live data, logging data, and sending them to an FTP server. The software code for both PC application and PLCs software is freely available at https://github.com/purrutti/CocoriCO2.

An ethernet switch allows the communication between the PLCs and the computer, and an internet connection to allow remote control and monitoring. If communication with the monitoring computer is lost, the PLCs continue to regulate the installation. The master PLC also holds an SD card on which all the measures and regulation data are stored in case communication with the computer is lost.

## Human–machine interface

### *Experiment monitoring*

On the computer, the main window of the interface (Fig. 6A) shows the 12 tanks and their piping connections. It also shows two general seawater inlets (ambient and warmed). At the bottom of the window, a status bar shows the current connection status (connection with the PLCs), and the date and time of the last communication packet received from the master PLC (every minute). On the left is shown the pressure set points and the pressure measures for each seawater inlet. The valve opening percentage is also shown. The box on the left shows the measured ambient conditions.

For each tank, flow rate (L $min^{-1}$), pH, and temperature (°C) are shown. Temperature mixing valve and freshwater valve openings are also shown. pH measure, set point, and valve opening for the acidified tank is displayed on the left. pH and temperature measures and set points are shown on each mixing tank, as well as the temperature valve opening (in %) and the peristaltic pump flow rate (in %). At the top, the day/night status and times, as well as the high-/low-tide status and times, are displayed along with the current date and time. Finally, under "Maintenance," the regulation system can be paused by clicking on "Cleanup mode" when tanks are emptied for cleaning purposes.

### *Parameters tuning*

The principle of the regulation procedure relies on setting a value for offsets compared with ambient measurements. A window of the user-interface (Fig. 6B) allows to tune these

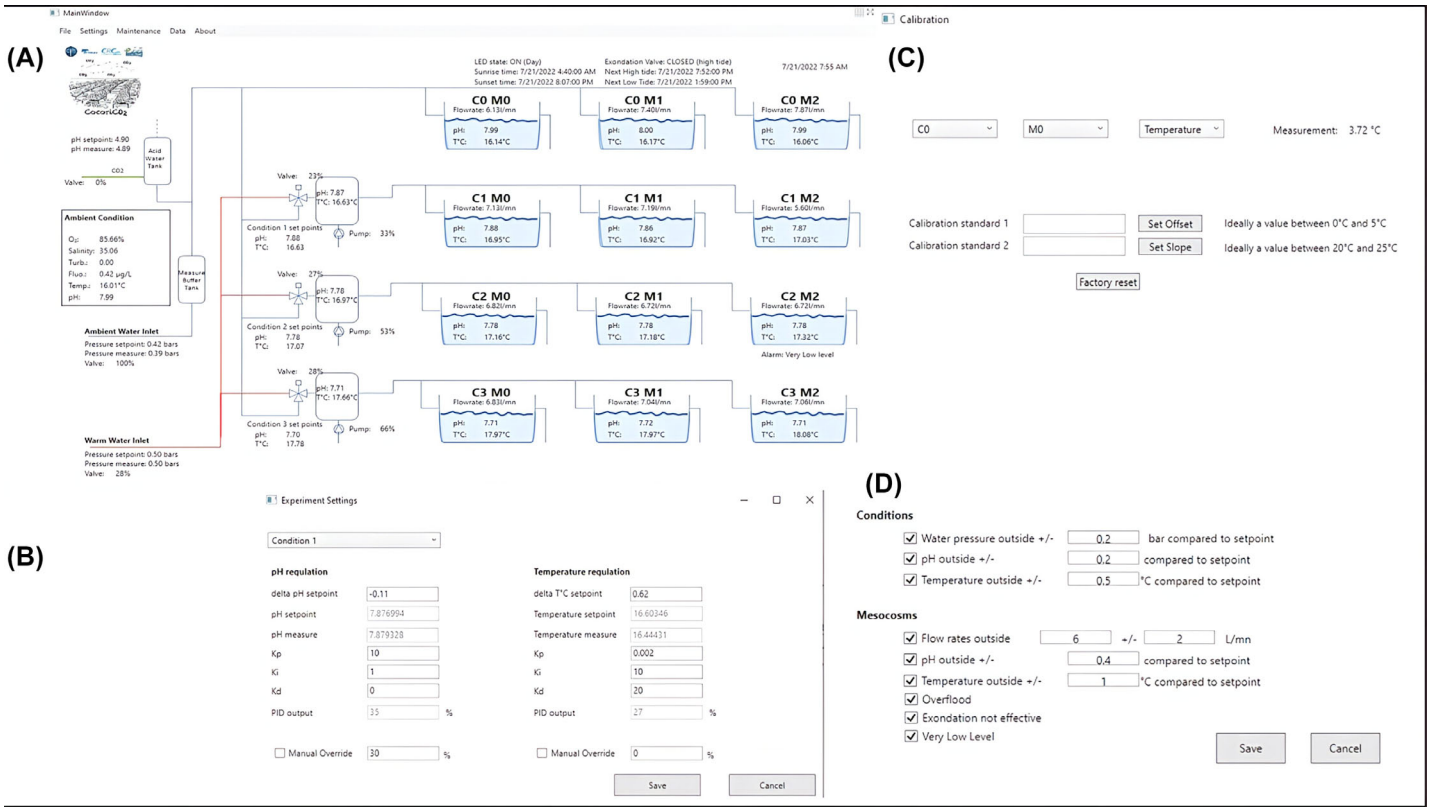


**Fig. 6.** Software interface (**A**: main window, **B**: experiment settings, **C**: sensor calibration, and **D**: alarm settings).

set points as well as to set the $K_p$ (proportional gain), $K_i$ (integral gain) and $K_d$ (derivative gain) parameters for the PID software regulator. Note that these parameters were fixed during the first few days of the testing period to optimize the regulation and were not modified afterwards. It is also possible to override the regulation and set the valve openings to a specified value (between 0% and 100%).

### *Parameters calibration*

Another window allows the user to calibrate all sensors (Fig. 6C). Sensor calibration was performed on a bi-weekly basis. All 17 sensors for the measurement of temperature and pH were inter-calibrated using a glass combination electrode (Solitrode with Pt1000 temperature sensor, Metrohm©) connected to a mobile pH and temperature logger (913 pH Meter, Metrohm©) and calibrated on the total scale using TRIS buffer solutions with a salinity of 35 (provided by A. Dickson, Scripps Institution of Oceanography, San Diego). Note that no drift was observed for temperature during the whole testing period. The conductivity sensor was inter-calibrated against discrete measurements using a laboratory conductivity meter (SevenEasy S30K, Mettler Toledo©) equipped with a Inlab 731 electrode (Mettler Toledo©) calibrated before each measurement against 50 mS $cm^{-1}$ standards (at 25°C). The fluorescence sensor was verified (no drift observed during the testing period) using a solid secondary standard (Turner Designs©) for which a correlation with discrete chlorophyll *a* (Chl *a*) measurements was established at the start of the testing period. A two-point calibration was used for the oxygen sensor that was plunged: (1) in an oxygen-free environment (freshwater with addition of sodium sulfite) and (2) in a 100% oxygen (air-bubbled seawater). As already mentioned, the turbidity sensor provided unreliable results and no calibration was further done after a few weeks of testing.

### *Data processing and visualization*

All the data from the experiment (measures, set points, regulation outputs) are saved on the master PLC SD card. It is also saved on the computer, and sent to an ftp server for remote access. Data can be visualized in two ways: (1) an influxDB server, installed on each computer running the application, receives and displays data every minute; and (2) a publicly available HTML webpage updated every hour (https://www.obs-vlfr.fr/~gazeau/CocoriCO2/CRCBN/CocoriCO2_CRCBN.html). The data are also stored on the computer and allows fast and easily configurable dashboards to display the past and present data. It is therefore used for live monitoring.

### *Alarm system*

An alarm system is set up to warn the operator in charge of the experiment that a measure is out of bounds. In the alarm settings window (Fig. 6D), the user can choose to

activate and set the thresholds for ambient and warmed water pressure, pH, temperature, flow rates, and seawater level. If an alarm is triggered, it is displayed in the alarm list window and sent to a dedicated slack (https://slack.com/) channel to alert the user.

## Results and discussion

### Quality assessment of the hydraulic system

Containers were deployed approximatively at the same time on both sites and were used for testing purposes. Unfortunately, we had to stop this testing in the Mediterranean after few weeks due to a problem with seawater supply. A new pumping system has been installed in summer 2022 and we were ready to restart the experimental system in October 2022. However, due to this imposed delay, we have decided not to restart a testing phase, already performed and successful in Brittany, but directly start an experiment on mussels and cupped oysters. This is the reason why most data presented in this section come from the testing phase in Brittany where the experimental system operated continuously between 14 January 2022 and 30 September 2022, that is, 260 d. During this period, there were minor outages on 17 non-consecutive days (or 6.5% of the time), which were primarily caused by pressure leaks. Fixing these breakdowns required shutting off the water supply, draining the tanks, and carefully relocating the animals away from the water to prevent their exposure to toxins (e.g., accumulation of ammonium) and lowering pH/oxygen levels. Communication between the master PLC and the computer was sometime interrupted, but all the data were recovered from the SD card of the master PLC. During the entire test period, there was no failure on the seawater pump or the heat pump. The ambient seawater pressure was maintained remarkably constant at 40,000 Pa (data not shown). The pressure of the warm seawater (data not shown) was more variable than that of the ambient pressure possibly due to upstream usage (i.e., other rearing activities in the facilities of the CRCBN), yet it did not affect the temperature regulation (*see* thereafter). Seawater flow rates were very similar between tanks and rather constant during the entire test period (Table 2). Finally, the valve system to partially empty tanks at low tide was very efficient. The instances where one or more tanks failed to drain, primarily due to miscommunications or a valve blockages, did not exceed 8.5% of the test phase. This value is an overestimation, as on many occasions, the issue came from blockages of one or more float level switches. These switches failed to signal the system but did not reflect a malfunction in the drainage valve.

**Table 2.** Average and standard deviations (SD) of seawater flow rates delivered to the mesocosms (a, b and c) for the different treatments (2022, 2050, 2075, and 2100) during the testing period in Brittany (14 January 2022 to 30 September 2022).

| | Flow rate (L $min^{-1}$) | |
|---|---|---|
| Treatment | Average | SD |
| 2022-a | 6.45 | 0.92 |
| 2022-b | 6.67 | 0.76 |
| 2022-c | 6.94 | 0.71 |
| 2050-a | 6.76 | 0.94 |
| 2050-b | 6.75 | 0.85 |
| 2050-c | 6.56 | 0.82 |
| 2075-a | 6.71 | 0.92 |
| 2075-b | 6.77 | 0.67 |
| 2075-c | 6.65 | 0.89 |
| 2100-a | 6.99 | 0.61 |
| 2100-b | 6.75 | 0.98 |
| 2100-c | 6.88 | 0.56 |

### Representativeness of control seawater vs. ambient conditions

The general objective behind developing these experimental systems was to allow conducting perturbation experiments under conditions as close to real-life as possible. The high turnover rate of seawater within the tanks (i.e., renewing the entire seawater volume every 30 min) was specifically selected based on animal densities. This choice serves multiple purposes: (1) to minimize the impact of reared animals on seawater chemistry, including oxygen consumption, ammonium accumulation, and undesirable pH changes; (2) to limit heat exchange between tank seawater and the atmosphere, maintaining temperature closer to those recorded at the entrance of the container; and (3) to ensure adequate food availability for organisms, mimicking observed growth rates in natural settings.

Figure 7 presents daily differences in terms of both temperature and pH between the values measured in the triplicate control (i.e., 2022) tanks (with animals) and ambient levels.

Temperature differences were on average $0.08 \pm 0.08$°C (mean $\pm$ SD) with minimal and maximal values of $-0.14$°C and 0.40°C, respectively. These values are well below the temperature offset applied for the 2050 treatment (0.6–0.8°C, Table 1). In one of the control tanks (2022-b), temperature levels slightly but consistently trended higher compared with the other two tanks (Fig. 7). It is likely that air mixing was not optimal. This will be solved by adding fans at the outlet of the perforated air-conditioning channel.

Differences in pH between ambient and control seawater were on average $0.00 \pm 0.02$ pH units with minimal and maximal values of $-0.07$ and $+0.09$ pH units. As for temperature, these values are well below the pH offset applied for the 2050 treatment ($\sim -0.1$ pH units). Discrepancies in pH values between ambient and control seawater could potentially stem from respiration and calcification of organisms and/or irregularities in the pH probe calibration, which was conducted every 2 weeks. This was fixed as soon as important differences were observed among the triplicate tanks.

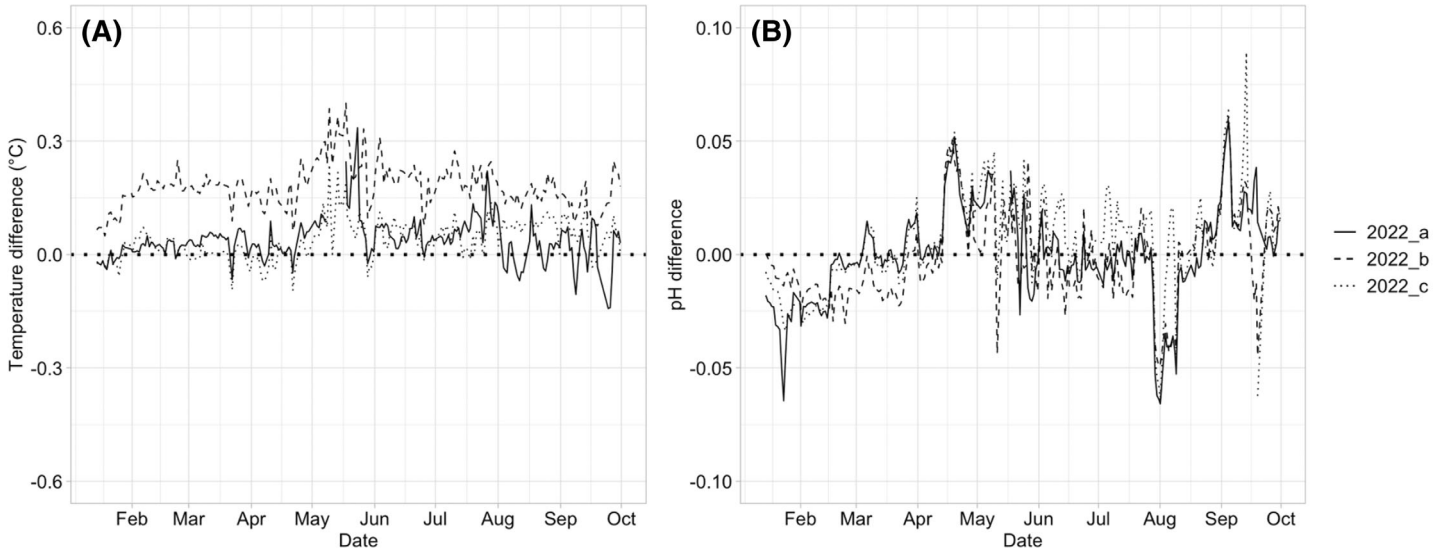


**Fig. 7.** Temperature (**A**) and pH (**B**) differences in the three rearing tanks (a, b, and c) from the 2022 condition (i.e., control) as compared with ambient conditions during the testing period (14 January 2022 to 30 September 2022) in Brittany.

Considering the significance of food and energy availability in projecting the future impact of environmental drivers on marine organisms, a crucial step involves adapting the density of reared animals to the flow of seawater to ensure there is no food limitation as well as comparing growth rates of specimens maintained in the container to those in their natural field habitats. During the study conducted in the Mediterranean from October 2022 to September 2023, around 400 individuals of each species (37 and 13 mm shell length for cupped oysters and Mediterranean mussels, respectively) corresponding to a biomass (total fresh weight) of 2400 ± 80 for oysters and 66 ± 83 g for mussels were introduced to the tanks at the start of the experiment. This number of specimens was calculated as to allow enough sampling material during the experiment and to ensure that total filtration rates of the organisms, based on temperature- and size-dependent published individual filtration rates, never surpass the flow of seawater provided to each tank. To verify this assumption, growth rates of Pacific oysters maintained in the control tanks and of specimens taken from the same initial cohort and deployed in situ in Marseillan, France (43.39°N, 3.47°E, 5 km

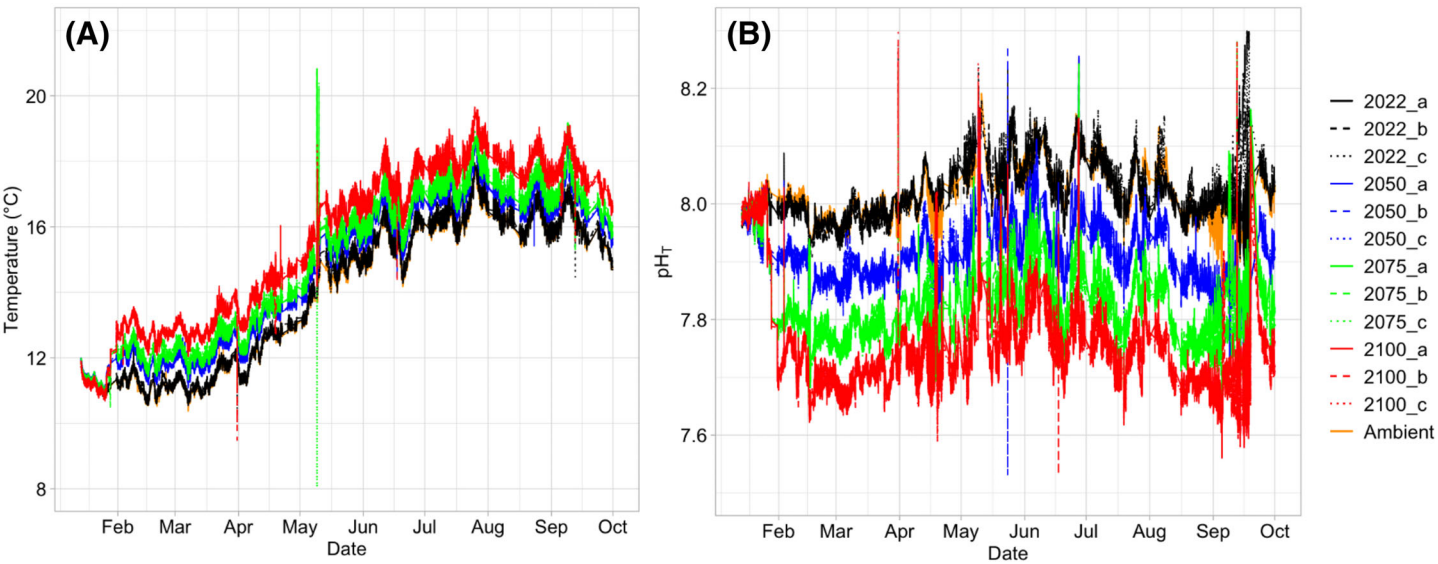


**Fig. 8.** Raw (i.e., every minute) temperature (**A**) and pHT (pH on the total scale; **B**) measurements in the triplicate rearing tanks (a, b, and c) for each condition (2022, 2050, 2075, and 2100) as well as at the entrance of the container (ambient) during the testing period (14 January 2022 to 30 September 2022) in Brittany.

from the container at a depth of 4.5 m) were compared. This comparison presented in Supporting Information Fig. A.4 revealed no significant differences in terms of growth which implies that the rearing conditions in the container under control conditions were fully realistic.

### Temperature and pH regulation

Throughout the testing period in Brittany, the regulation of temperature and pH in the different treatment conditions (2050, 2075, and 2100) was maintained for 9 months by the experimental system (Fig. 8). At the onset of the testing period on 12 January 2022, the treatment conditions mirrored ambient settings for the first 2 weeks. Then, starting on 26 January 2022, a programmed adjustment induced a gradual temperature increase and pH reduction to reach the targeted levels for each condition by 03 February 2022.

The daily offsets from control condition (daily average of raw data collected every minute) as well as hourly averaged data are presented in Fig. 9 and are further averaged (± SD) over the whole duration of the test period in Brittany in Table 3. Targeted offsets were maintained in the mixing tanks with average deviation from the nominal values of less than 0.2°C and 0.01 pH units over the entire period demonstrating a very good capacity of our system to simulate the three perturbed experimental conditions.

These offsets measured in the mixing tanks were well reproduced in the rearing tanks (Fig. 10). Differences between nominal and measured offsets were maximal in the 2050 treatment for temperature (Table 3). On average, the measured temperature offset for this treatment was 0.13–0.18°C higher than the +0.62°C nominal offset. While the regulation in the mixing tank seemed effective and the seawater flow rates did not significantly differ from those in other treatments, the specific reasons behind this deviation are not yet fully understood. The level of pH in all tanks were in very good agreement with the nominal conditions, except on very few occasions due to improper calibration or inadvertent air-exposure of the pH probe for few hours (Fig. 10). Overall, the measured pH in the tanks showed deviation of less than 0.03 pH units from the nominal values (Table 3), which is well below the pH offsets considered for the different treatments (Table 1).

**Table 3.** Mean temperature (°C) and pH differences (± SD) between measured and nominal values for the three different perturbation treatments (2050, 2075, and 2100) in the corresponding mixing tanks and in the triplicate mesocosms (a, b, and c) during the testing period in Brittany (14 January 2022 to 30 September 2022).

| Conditions | Mean temperature difference | Mean pH difference |
|---|---|---|
| 2050 (mixing tank) | 0.08 ± 0.08 | 0.01 ± 0.01 |
| 2050-a | 0.13 ± 0.12 | 0.02 ± 0.04 |
| 2050-b | 0.14 ± 0.09 | 0.02 ± 0.02 |
| 2050-c | 0.18 ± 0.09 | 0.02 ± 0.02 |
| 2075 (mixing tank) | 0.15 ± 0.12 | 0.01 ± 0.02 |
| 2075-a | 0.10 ± 0.13 | 0.03 ± 0.06 |
| 2075-b | 0.14 ± 0.12 | 0.02 ± 0.04 |
| 2075-c | 0.14 ± 0.12 | 0.02 ± 0.04 |
| 2100 (mixing tank) | 0.18 ± 0.15 | 0.01 ± 0.02 |
| 2100-a | 0.07 ± 0.11 | 0.02 ± 0.05 |
| 2100-b | 0.11 ± 0.26 | 0.02 ± 0.03 |
| 2100-c | 0.11 ± 0.35 | 0.02 ± 0.03 |

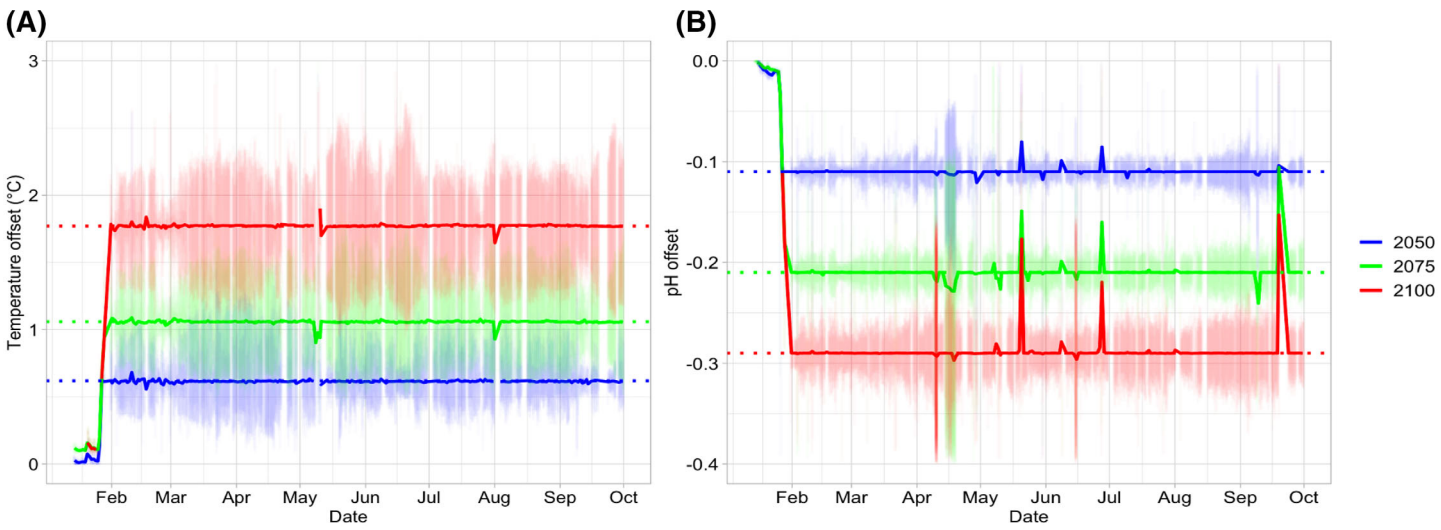


**Fig. 9.** Temperature (**A**) and pH (**B**) offsets in the three mixing tanks (conditions simulated for 2050, 2075, and 2100) as compared to ambient conditions during the testing period (14 January 2022 to 30 September 2022) in Brittany. Thick solid lines present daily average values while transparent thin lines present hourly data. Targeted offsets are represented by horizontal dotted lines (*see* Table 1).

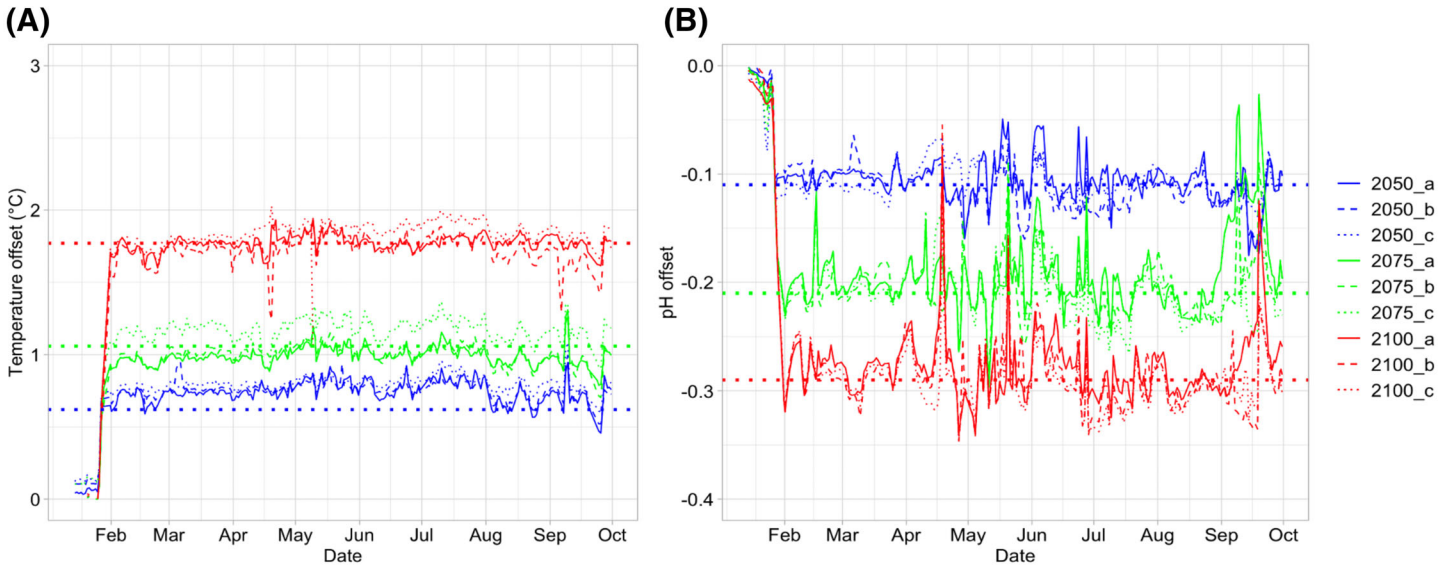


**Fig. 10.** Temperature (**A**) and pH (**B**) offsets (hourly data) in the triplicate rearing tanks (a, b, and c) for each perturbed treatment (2050, 2075, and 2100) as compared with ambient conditions, during the testing period (14 January 2022 to 30 September 2022) in Brittany. Targeted offsets are represented by horizontal dotted lines (*see* Table 1).

### Potential effect of warmed and acidified water on food availability

Our experimental systems were designed to minimize the impact of seawater treatment (warming and acidification) on food availability, a critical factor that influence growth, survival, and reproduction of marine organisms. As such, it was decided not to prefilter seawater before its delivery to the heat pump or to the acidified tank to avoid decreasing the amount of particulate organic matter, and therefore food availability at varying degrees across the treatments. This choice to limit phytoplankton dilution was made at the expense of a more intense maintenance effort (i.e., cleaning the heat exchanger once a week). However, acidifying seawater to very low level of pH as produced in the acidified tank could significantly impact phytoplankton leading to a decrease in viable cells in the acidified water delivered to the tanks. The same is true for warming as heating phytoplankton to up to 45°C (maximum seawater produced by the heat pump) could significantly alter them. To limit this potential experimental bias, we aimed to limit the proportion of acidified and warmed water with respect to ambient seawater.

Regarding acidification, we worked with acidified seawater close to $CO_2$ saturation (i.e., pH = 4.9; Supporting Information Fig. A.2) to proceed only with very small addition of acidified seawater to decrease pH in the mixing tanks. Considering this, a mere 0.15% of saturated seawater is required to lower the pH by 0.1 units at an average temperature of 14°C, a salinity of 34, and a $pH_T$ of 8.02 corresponding to average values during the testing period in Brittany. For the most acidified treatment (pH offset of ∼ −0.3), this amounts to the addition of 0.45% of $CO_2$-enriched seawater.

Likewise, in an effort to reduce the influx of warm water into the mixing tank, the heat exchanger was set to high-temperature levels (at least 10°C above ambient levels). Specifically, during the experiment held at the Mediterranean site starting in October 2022, we maintained temperature between 40°C and 45°C for fall/winter and spring/summer periods, respectively. Considering ambient temperature and nominal offsets (Table 1), 3–4%, 6–8%, and 10–12% of heated seawater were required to reach the nominal temperature offsets for 2050, 2075, and 2100, respectively.

Finally, we verified that the addition of acidified and warmed seawater did not alter food availability. To achieve this, we conducted repeated samplings at the Mediterranean site during the experiment conducted from October 2022 to December 2023, evaluating the Chl *a* content in each tank (while removing the animals) to assess potential scenario effects on food availability. The results indicate no significant effect (*see* results obtained in June 2023, Supporting Information Fig. A.5, Kruskal–Wallis test, $p = 0.103$).

## Conclusions and perspectives

The experimental units developed as part of the Cocori$CO_2$ project have shown their effectiveness in terms of controlling and maintaining pH and temperature as offsets from natural conditions to assess the future of mollusk farming under the pressure of ocean warming and acidification. Similar systems have been developed in the past years to expose plants/macroalgae and/or invertebrates to changing and fluctuating temperature and pH conditions (e.g., Duarte et al. 2015; Wahl et al. 2015; Falkenberg et al. 2016; Pansch and Hiebenthal 2019).

Besides having proven its viability and efficiency to accurately control these parameters for a much longer period of time than these existing facilities (tested for a few weeks to a few months), the main advantage of our experimental units resides in the fact that they are fully integrated in shipping containers which offers the advantage of being easily transportable to a study site and even to be embarked on a research vessel. Our systems have been initially developed to study the response of benthic invertebrates to environmental changes which does not necessitate exposure to natural light. However, with relatively few adaptations, they could be used to study the response of photosynthetic organisms to warming and acidification through the installation of outdoor tanks at the vicinity of the container.

Regarding the perturbation protocol, it was decided at the start of the project to consider a scenario approach, that is, combining warming and acidification to project the conditions at different time scales in each area. However, it must be stressed that, while this approach is interesting to provide relevant information to shellfish growers regarding the future of their activity, our experimental systems are easily adaptable to consider different experimental protocols that allow discriminating the impacts of warming and acidification.

Similarly, it is important to note two potential limitations regarding the chosen experimental protocol. The first limitation is that the rearing tanks are not true replicates. A single mixing tank supplies three rearing tanks, making these tanks pseudo-replicates (Cornwall and Hurd 2016). If a mixing tank corresponding to a particular condition or scenario is influenced by an unintended factor (referred to as "the demon" or more seriously "confounder" by Hurlbert in his seminal paper on the subject; Hurlbert 1984), there is a risk that this factor and the scenario may interact unpredictably.

In our case, we believe this is not a significant concern for two reasons. First, the experiments conducted using this setup are meant to be long term, reducing the likelihood that a confounding factor in one of the mixing tanks will have a significant impact over time. Additionally, the risk of confounding factors can be mitigated by alternating the scenarios across different tanks over time. Second, the experimental design includes two independent and identical containers, which allow testing the impact of environmental scenarios in two contrasted environments. This approach offers the potential for replication at a regional level, which we believe is much more relevant than making the experimental units within each container completely independent.

The second limitation of the system is its reliance on triplicates. If a tank is accidentally lost, the number of experimental units would become insufficient for statistical analysis. Even without such an incident, the statistical power remains minimal. However, again since the experiments are designed to be long term, it is expected that the observed differences will become more pronounced over time, compared with short-term experiments. In the event that additional replicates are necessary, the experimental system is sufficiently flexible, within the limits of fitting all equipment inside a shipping container, to increase their number by considering smaller tank sizes or decreasing the number of treatments without compromising its overall functionality.

Finally, our project was focused on two environmental factors that are known to impact mollusk physiology, but they are not the only ones. Ocean deoxygenation poses a very serious threat to shellfish production, especially in enclosed bays, estuaries, or lagoons. Precipitations and freshwater runoff are also projected to change in the coming decades leading to exposition of mollusks to varying conditions in terms of salinity. Our system with minimal adaptation (e.g., addition of $N_2$ gas to decrease oxygen levels, addition of freshwater and salt to decrease and increase salinity, respectively) could be a valuable tool to provide an educated assessment of the future of shellfish farming under these environmental changes.

## References


Albright, R., and others. 2018. Carbon dioxide addition to coral reef waters suppresses net community calcification. Nature **555**: 516–519. doi:10.1038/nature25968

Barton, A., B. Hales, G. G. Waldbusser, C. Langdon, and R. A. Feely. 2012. The Pacific oyster, *Crassostrea gigas*, shows negative correlation to naturally elevated carbon dioxide levels: Implications for near-term ocean acidification effects. Limnol. Oceanogr. **57**: 698–710. doi:10.5194/acp-15-7961-2015

Barton, A., and others. 2015. Impacts of coastal acidification on the Pacific Northwest shellfish industry and adaptation strategies implemented in response. Oceanography **25**: 146–159. doi:10.5670/oceanog.2015.38

Bednaršek, N., and others. 2021. Synthesis of thresholds of ocean acidification impacts on echinoderms. Front. Mar. Sci. **8**: 602601. doi:10.3389/fmars.2021.602601

Carstensen, J., and C. M. Duarte. 2019. Drivers of pH variability in coastal ecosystems. Environ. Sci. Technol. **53**: 4020–4029. doi:10.1021/acs.est.8b03655

Cornwall, C. E., and C. L. Hurd. 2016. Experimental design in ocean acidification research: Problems and solutions. ICES J. Mar. Sci. **73**: 572–581. doi:10.1093/icesjms/fsv118

Duarte, G., E. N. Calderon, C. M. Pereira, L. F. B. Marangoni, H. F. Santos, R. S. Peixoto, A. Bianchini, and C. B. Castro. 2015. A novel marine mesocosm facility to study global warming, water quality, and ocean acidification. Ecol. Evol. **5**: 4555–4566. doi:10.1002/ece3.1670

Falkenberg, L. J., B. D. Russell, and S. D. Connell. 2016. Design and performance evaluation of a mesocosm facility and techniques to simulate ocean acidification and warming. Limnol. Oceanogr. Methods **14**: 278–291. doi:10.1002/lom3.10088

FAO. 2022. The state of world fisheries and aquaculture 2022. Towards Blue Transformation. doi:10.4060/cc0461en

Friedlingstein, P., and others. 2022. Global carbon budget 2022. Earth Syst. Sci. Data **14**: 4811–4900. doi:10.5194/essd-14-4811-2022

Froehlich, H. E., R. R. Gentry, and B. S. Halpern. 2018. Global change in marine aquaculture production potential under climate change. Nat. Ecol. Evol. **2**: 1745–1750. doi:10.1038/s41559-018-0669-1

Gattuso, J. P., and others. 2015. Contrasting futures for ocean and society from different anthropogenic $CO_2$ emissions scenarios. Science **349**: 45. doi:10.1126/science.aac4722

Gazeau, F., L. M. Parker, S. Comeau, J.-P. Gattuso, W. A. O'Connor, S. Martin, H.-O. Pörtner, and P. M. Ross. 2013. Impacts of ocean acidification on marine shelled molluscs. Mar. Biol. **160**: 2207–2245. doi:10.1007/s00227-013-2219-3

Gibbs, M. C., L. M. Parker, E. Scanes, M. Byrne, W. A. O'Connor, and P. M. Ross. 2021. Adult exposure to ocean acidification and warming remains beneficial for oyster larvae following starvation. ICES J. Mar. Sci. **78**: 1587–1598. doi:10.1093/icesjms/fsab066

Hofmann, G. E., and others. 2011. High-frequency dynamics of ocean pH: A multi-ecosystem comparison. PLoS One **6**: e28983. doi:10.1371/journal.pone.0028983

Hurlbert, S. H. 1984. Pseudoreplication and the design of ecological field experiments. Ecol. Monogr. **54**: 187–211. doi:10.2307/1942661

IPCC. 2023. Climate change 2023: Synthesis report. *In* Core Writing Team, H. Lee, and J. Romero [eds.], Contribution of Working Groups I, II and III to the Sixth Assessment Report of the Intergovernmental Panel on Climate Change. IPCC. doi:10.59327/IPCC/AR6-9789291691647

Kroeker, K. J., R. L. Kordas, R. Crim, I. E. Hendriks, L. Ramajo, G. S. Singh, C. M. Duarte, and J.-P. Gattuso. 2013. Impacts of ocean acidification on marine organisms: Quantifying sensitivities and interaction with warming. Glob. Chang. Biol. **19**: 1884–1896. doi:10.1111/gcb.12179

Kwiatkowski, L., and others. 2020. Twenty-first century ocean warming, acidification, deoxygenation, and upper-ocean nutrient and primary production decline from CMIP6 model projections. Biogeosciences **17**: 3439–3470. doi:10.5194/bg-17-3439-2020

Lim, Y.-K., X. Dang, and V. Thiyagarajan. 2021. Transgenerational responses to seawater pH in the edible oyster, with implications for the mariculture of the species under future ocean acidification. Sci. Total Environ. **782**: 146704. doi:10.1016/j.scitotenv.2021.146704

Narita, D., K. Rehdanz, and R. S. J. Tol. 2012. Economic costs of ocean acidification: A look into the impacts on shellfish production. Clim. Chang. **113**: 1049–1063. doi:10.1007/s10584-011-0383-3

Pansch, C., and C. Hiebenthal. 2019. A new mesocosm system to study the effects of environmental variability on marine species and communities. Limnol. Oceanogr. Methods **17**: 145–162. doi:10.1002/lom3.10306

Stewart-Sinclair, P. J., K. S. Last, B. L. Payne, and T. A. Wilding. 2020. A global assessment of the vulnerability of shellfish aquaculture to climate change and ocean acidification. Ecol. Evol. **10**: 3518–3534. doi:10.1002/ece3.6149

Vargas, C. A., and others. 2017. Species-specific responses to ocean acidification should account for local adaptation and adaptive plasticity. Nat. Ecol. Evol. **1**: 1–7. doi:10.1038/s41559-017-0084

Wahl, M., and others. 2015. A mesocosm concept for the simulation of near-natural shallow underwater climates: The Kiel Outdoor Benthocosms (KOB). Limnol. Oceanogr. Methods **13**: 651–663. doi:10.1002/lom3.10055

Zhao, L., and others. 2020. A review of transgenerational effects of ocean acidification on marine bivalves and their implications for sclerochronology. Estuar. Coast. Shelf Sci. **235**: 106620. doi:10.1016/j.ecss.2020.106620

Ziegler, J. G., and N. B. Nichols. 1942. Optimum settings for automatic controllers. Trans. ASME **64**: 759–768. doi:10.1115/1.4019264

## Acknowledgments

The authors thank Benoît Salaun, Ricardo Gonzáles-Araya, Corentin Chevalier and Martin Protat from the Comité Régional de la Conchyliculture de Bretagne Nord (CRCBN) as well as Patrice Lafont, Fabrice Grillon-Gaborit, and Adeline Perignon from the Comité Régional de la Conchyliculture de Méditerranée (CRCM) for their participation at various stages of the project. Hervé Violette is thanked for his help during experiments in the field and at the container located in the Mediterranean site. Lester Kwiatkowski is thanked for providing regional projections of pH and temperature for the two study sites. This study was financially supported by the Cocori$CO_2$ project (European Maritime and Fisheries Fund, EMFF, 2020–2023).

*Submitted 31 January 2024*
*Revised 04 June 2024*
*Accepted 06 June 2024*

*Associate editor: Hayley Schiebel*